

Proceedings of the Seventh International Conference on Artificial Intelligence, Soft Computing, Machine Learning and Optimization, in Civil, Structural and Environmental Engineering Edited by: P. Iványi, J. Kruis and B.H.V. Topping Civil-Comp Conferences, Volume 11, Paper 2.2 Civil-Comp Press, Edinburgh, United Kingdom, 2025

ISSN: 2753-3239, doi: 10.4203/ccc.11.2.2

# MLP Neural Networks To Identify Damage in Bridges From SHM Data

A. Montisci<sup>1</sup>, F. Pibi<sup>2</sup> and M. C. Porcu<sup>2</sup>

<sup>1</sup>Dept. of Electrical and Electronic Engineering, University of Cagliari, Italy

<sup>2</sup>Department of Civil, Environmental Engineering and Architecture, University of Cagliari, Italy

#### **Abstract**

Multi-layer perceptron neural networks may be applied to improve structural health monitoring of existing structures. The present paper presents a preliminary application of a MLP neural network-based procedure to identify damage scenarios of concrete bridges. Reference was made to the well-known benchmark Z24 bridge, where full-scale different damage scenarios (such as pier settlement, concrete spalling and tendon rupture) were progressively produced on purpose. The proposed methodology trains MLP neural networks on databases of experimental acceleration time histories and classifies each damage type based on the frequency response spectrum. The results show the likely ability of MLP networks to categorize different kinds of structural damage in existing bridges, thereby contributing to advancements in automated structural health monitoring.

**Keywords:** artificial neural networks, machine learning, multi-layer perceptron, structural health monitoring, damage identification, concrete bridges.

### 1 Introduction

Aging, environmental factors, and fatigue effects due to cyclic loads may affect the serviceability and safety of bridges. Standard techniques based on structural health monitoring (SHM) are often used to detect damage in this kind of constructions [1,2,3,4]. However, the huge amount of data to process and interpret may call for automation and real-time analysis procedures. Recently, this matter has been addressed through artificial intelligence (AI) [5]. In particular, artificial neural

network (ANN) techniques, which are becoming commonly used in civil engineering [6], could be exploited to automatize damage detection through SHM.

This paper aims to investigate the application of a multi-layer perceptron (MLP) ANN to identify different types of damage in concrete bridges. To this purpose, reference to the benchmark database of the controlled progressive damage tests carried out on the highway post-tensioned concrete Z24 Bridge [7] is made. Referring to this famous vibration dataset, previous studies implemented machine-learning approaches to identify damage. Among them, convolutional neural networks (CNNs) [8,9] and k-nearest neighbour (KNN) [10] were exploited. Moreover, deep neural networks [11] and hybrid methods combining ANN with autoregressive models [12] were applied to detect damage scenarios of the Z24 Bridge.

The novelty of the present approach relies on the use of MLP neural networks, which are the simplest neural structures that can be used to classify non-linearly separable sets. One of their main advantages lies in the lower computational burden compared to other neural network architectures (e.g., the learning vector quantification [13]) that could be used for damage classification purposes [14,15,16]. This study aims to investigate the ability of the simple MLP classifier to identify the presence of damage in bridges and categorize its nature. The results of this investigation can give important indications for future work and provide a major advance in health monitoring and damage detection in bridges.

The paper is organized as follows. A brief description of the Z24 benchmark case is provided in Section 2, where the different experimental damage setups are recalled, according to [7]. Section 3 describes the adopted methodology, based on a preliminary pre-processing of data and successive training of an MLP for each experimental setup. The results are provided in Section 4, while some conclusive remarks are given in Section 5.

# 2 Z24 bridge benchmark database

### **2.1 Z24** bridge

The Z24 bridge (Figure 1) was a three-span post-tensioned concrete box-girder bridge located in Switzerland, near Solothurn (Bern) [7].



Figure 1: Archive picture of the Z24 bridge [7].

Entered service in 1963, it had a total length of 58 meters, with a main span of 30 meters and two side spans of 14 meters each (Figure 2a). The superstructure consisted

of a two-cell closed box girder with tendons in the three webs; the main piers (Pier 1 and Pier 2 in Figure 2a) were concrete diaphragms and the abutments consisted of triple concrete columns connected with concrete hinges to the girder (Figure 2b). Due to the need for a new bridge to accommodate the developing railway infrastructure, the bridge was demolished in 1998.

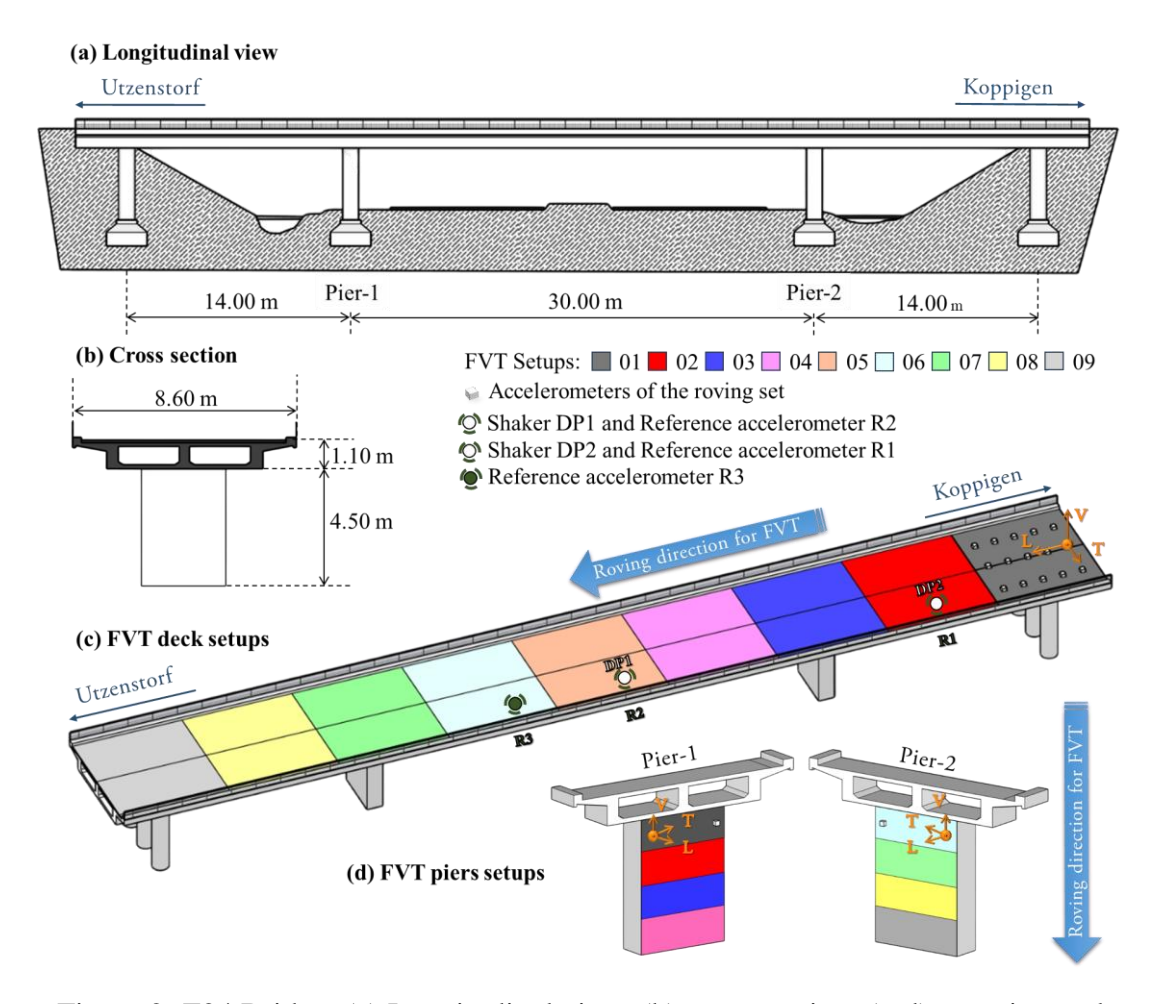


Figure 2: Z24 Bridge. (a) Longitudinal view; (b) cross section; (c-d) experimental setups for the PDs under the Forced Vibration Tests (FVTs) [17].

# 2.2 Database of the progressive damage tests

Before its demolition, the Z24 bridge was tested under full scale different damage scenarios to provide an experimental basis for evaluating the feasibility of using vibration-based SHM methods to identify damage from changes in the bridge's dynamic characteristics.

In the framework of the SIMCES (System Identification to Monitor Civil Engineering Structures) project [18], the bridge was extensively instrumented with different kinds of sensors. The 17 short-term controlled progressive damage (PD) scenarios listed in Table 1 were considered [17,19].

The PDs in Table 1 can be divided into 8 main categories. To the first category belong the reference scenarios PD-1, PD-2 and PD-8. Scenario PD-1 is relevant to the undamaged condition.

Id	Damage scenario	Damage feature
PD-01	1° reference measurement	Undamaged
PD-02	2° reference measurement	Installation of pier settlement system
PD-03	Lowering of pier, 20 mm	Reversible
PD-04	Lowering of pier, 40 mm	Reversible
PD-05	Lowering of pier, 80 mm	Reversible
PD-06	Lowering of pier, 95 mm	Reversible
PD-07	Lifting of pier, tilt of foundation of 0.5 degrees	Reversible
PD-08	3° reference measurement, new condition	Restored pier
PD-09	Spalling of concrete at soffit, 12 m <sup>2</sup>	Irreversible
PD-10	Spalling of concrete at soffit, 24 m <sup>2</sup>	Irreversible
PD-11	Landslide of 1m at abutment	Irreversible
PD-12	Failure of concrete hinges	Irreversible
PD-13	Failure of 2 tendon anchor heads	Irreversible
PD-14	Failure of 4 tendon anchor heads	Irreversible
PD-15	Rupture of 2 out of 16 tendons	Irreversible
PD-16	Rupture of 4 out of 16 tendons	Irreversible
PD-17	Rupture of 6 out of 16 tendons	Irreversible

Table 1: Progressive damage scenarios on Z24 bridge.

PD-2 refers to the installation of the settlement system in Pier 2 (the pier was cut horizontally, and six hydraulic jacks were inserted). The initial condition of Pier 2 was restored in the third reference scenario PD-08. The second category includes the reversible settlements scenarios PD-3, PD-4, PD-5, PD-6, where Pier 2 was lowered in turn by 20 mm, 40 mm, 80 mm and 95 mm. The third category contains only one scenario: a 0.5-degree tilt of the Pier 2 foundation. The fourth category is relevant to concrete spalling: 12  $m^2$  and 15  $m^2$  spalling at soffit were considered respectively in the PD-9 and PD-10 irreversible scenarios. The fifth category considers the landslide irreversible scenario PD-11, simulated by removing some soil in between the triple columns at the Koppigen side abutment. The sixth category was about the failure of concrete hinges. The concrete hinges of the Koppigen triple columns were cut in the irreversible scenario PD-12. The seventh category included irreversible tendon-head rupture. The rupture of 2 and of 4 of the tendon anchor heads was considered in PD-13 and PD-14, respectively. The eight category was relevant to the tendon failure.

The rupture of respectively 2, 4 and 6 out of 16 tendons was produced in the irreversible scenarios PD-15, PD-16 and PD-17.

For each of the above-described PDs, both ambient vibration tests (AVTs) and forced vibration tests (FVTs) were carried out. The present study refers only to the FVTs. The FVTs were carried out by giving harmonic loads through two hydraulic shakers placed on the deck (in the positions DP1 and DP2 showed in Figure 2c) [17]. The first shaker (SCHENK POKK/N) was able to produce forces between ±5 kN in a frequency range 2.3 Hz ÷ 100 Hz; the second shaker (SCHENK PLz 25 N Q 160) could generate ±20 kN in the frequency range 1.5 Hz ÷ 60 Hz. The response was acquired by roving a set of 15 three-axial accelerometers along the deck, thus obtaining 9 different setups, referred to as 01, 02, ..., 09, and indicated with different colors in Figure 2c. The same setups included also a couple of three-axial accelerometers roved on Pier 1 and another couple roved on Pier 2 (see Figure 2d). In addition, three reference accelerometers were kept fixed in positions R1, R2 and R3 on the deck (Figure 2c). A triad with longitudinal (L), transversal (T) and vertical (V) directions is depicted in Figure 2c and Figure 2d at one on the deck and at one of the pier three-axial accelerometers, indicating the potential acquisition directions.

During the experimental campaign, synchronized signals were recorded from 34 channels [17,20], 33 of them corresponding to some accelerometer directions and the last one acquiring the shaker input. Figure 3 provides the relevant pattern of accelerometers. Each signal acquisition lasted 10.9 minutes and was sampled simultaneously at 100 Hz. Finally, each signal consisted of 65 536-time samples.

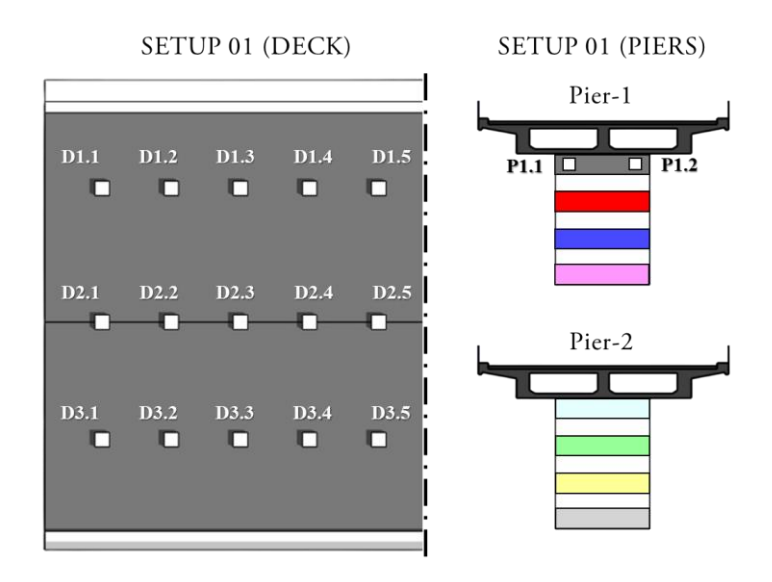


Figure 3: Pattern of accelerometers in Setup 01 [17].

Table 2 summarizes the correspondence between channels and positions/directions of sensors/shaker in Setup 01.

The signals acquired in the vertical direction by the deck accelerometer D3.1 (Setup 01) are plotted in Figure 4a, relevant to seven damage scenarios representative of the main PD categories (see Table 1).

Channel	Position (accelerometer/shaker)	Direction
from 1 to 5	D3.1, D3.2, D3.3, D3.4, D3.5	V
from 6 to 8	D2.1	L, T, V
from 9 to 10	D2.2	T, V
from 11 to 12	D2.3	T, V
from 13 to 14	D2.4	T, V
from 15 to 17	D2.5	L, T, V
from 18 to 22	D1.1, D1.2, D1.3, D1.4, D1.5	V
from 23 to 25	P1.1	L, T, V
from 26 to 28	P1.2	L, T, V
29	R1	V
from 30 to 32	R2	L, T, V
33	R3	V
34	DP2 (or DP1)	V
35 (optional)	DP1 (or DP2)	V

Table 2: Channels and position/directions in Setup 01.

Referring to the same setup and PDs, the signals acquired in the longitudinal direction L by the pier accelerometer P1.1 are plotted in Figure 4b. The comparison of the signals highlights the dissimilar dynamic behaviour of the bridge under the same loading conditions when different damage scenarios are concerned.

The difference between the response of the bridge in undamaged and damaged conditions is evident from the diagrams. However, it would be hard to distinguish between the seven couples of damaged signals and associate the correct scenario with each of them. Processing signals and suitably interpreting processed data is necessary to find out the category and severity of damage the structure is suffering. Based on MLP neural networks, the procedure described in the next section can be able to address this matter.

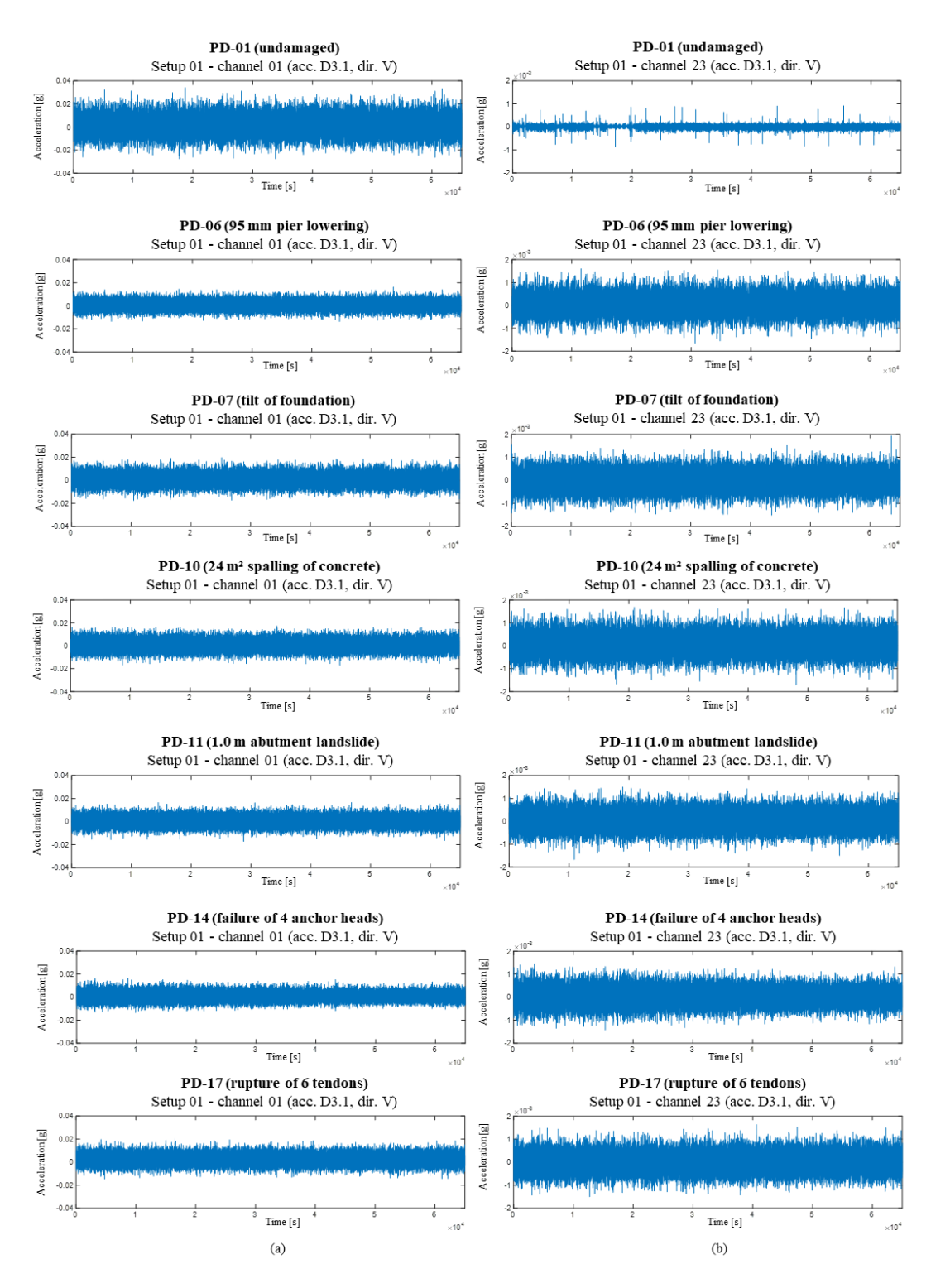


Figure 4: Examples of time-domain signals recorded by (a) deck accelerometer D3.1 and (b) pier accelerometer P1.1 in Setup 01 during 7 different PDs.

# 3 Methodology

The core of this research lies in utilizing the acceleration data acquired during the progressive damage tests on the Z24 bridge to train MLP neural networks to identify damage scenarios. A classification problem was thus defined, where each damage scenario represents a class. The process began with the creation of a dataset from the raw experimental data relevant to the 9 setups (Fig. 2c and 2d) and to the 17 PDs. Since signals belonging to different setups were not synchronized with each other, a specific MLP was trained for each setup. Therefore, 9 different diagnostic systems were developed. The set of diagnoses obtained from the different MLPs was finally combined with the majority voting criterion.

## 3.1 Data Pre-Processing

Processing of data was performed in Matlab [21] through the three steps presented in the following, (see Figure 5).

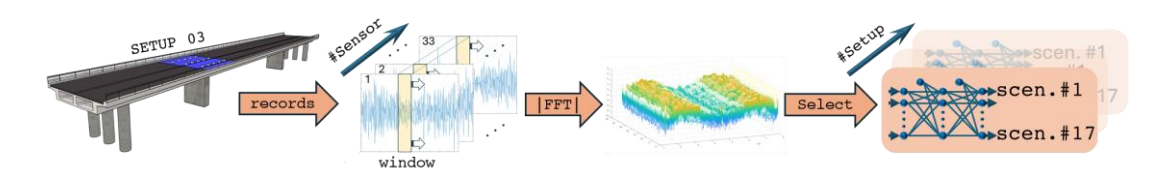


Figure 5: Scheme of the data pre-processing steps for a generic setup.

- STEP 1: For each given setup and PD, the signals (time sequences) acquired by each channel were subdivided into sliding windows of 4 000 samples, shifted with a 500 samples step, so that 123 windows for each sequence was retrieved. Synchronized time windows were collected from all the setups, by obtaining a 4 000×9 (samples × setups) matrix, which represents an instance of the dataset for each PD. The total number of instance matrixes was 123×17 (windows × PDs) = 2 091.
- STEP 2: The 2-dimensional fast Fourier transform (FFT) is applied to each instance matrix. Since the signals are not triggered, the phase of the frequency components was affected by uncertainty. Therefore, only the amplitude of the frequency components was considered.
- STEP 3: A selection of the frequency components is mandatory to make the training easier. To this end, a quality index, given by the ratio between the range of each class (damage scenario) and the range of the entire dataset, is calculated for each frequency component. The smaller the quality index the more suitable the frequency component to distinguish a class from the others. A ranking of quality indexes is defined for each class. The first 7 frequencies (K=7) of the ranking are considered to build the input pattern of the neural network, and finally the union of the selected frequencies (taken once) is used as an input pattern. The components of the input patterns are normalized to the interval [1, 1] by considering the range of values within the training set.

## 3.2 MLP training

An MLP neural network with variable structure X-10-17 is used as a classifier, where the output layer activation is a hyperbolic tangent function. Due to the variable dimension of the input pattern, the number of input neurons (X) may change from one setup to the other. The hidden layer was assumed equal to 10 for all the setups, while the output layer consisted of as many neurons as the number of classes (damage scenarios).

The number of training epochs was set to 1 000. However, in all cases the training stopped before reaching 1 000 epochs, due to minimum gradient or error rising in the validation set. Two independent random subsets made of 15% of the entire dataset of samples were used as validation and test set, respectively, while the complementary set to these two was used as training set. The performance of the system was evaluated on the test set. Several runs were performed, by selecting different validation and test subsets. In all training courses, the trend of the performance on both validation and test sets was close to that of the training set (see Figure 6). This means that both the training and validation sets are representative of the whole dataset, thus indicating that the distribution in the input space is well represented by all three subsets.

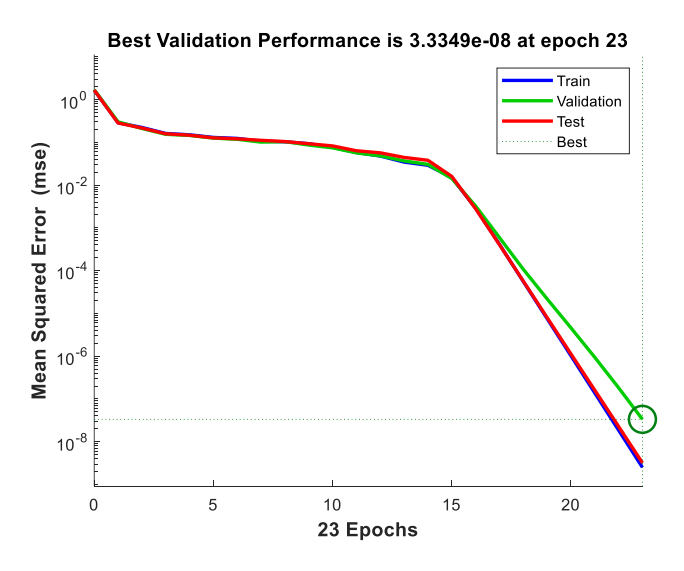


Figure 6: Performance diagram of the training set, validation set and test set.

### 4 Results and discussion

To check the effectiveness of the procedure, errors given by the difference between output and target values were calculated. The target for each damage scenario is a vector with as many components as the number of all scenarios, where to the current scenario is assigned the value 1 and to the others -1. Therefore, the absolute value of the threshold error leading to a misclassification was 1. A misclassification occurs when the difference between the target and the computed output (in absolute value) is greater than 1. Relevant to the test set and to the 9 setups, the maximum MLP error

of the 17 outputs for each example is shown in the diagrams of Figure 7. The results provided in the diagrams show that all MLPs were able to classify 100% of the test examples correctly. Only the MLP corresponding to Setup 07 did not have the same margin as in all the other cases, although the error was far from the misclassification threshold. It can be noted that the error was always negligible in 8 over the 9 setups. For Setup 07, an error of -0.4 was found at one instant (see Figure 4), which means that the output indicating the scenario was 0.6 instead of 1 (target value). On the other hand, the diagnosis indicated clearly the correct scenario, as the other components of the output were near to -1 (error almost zero).

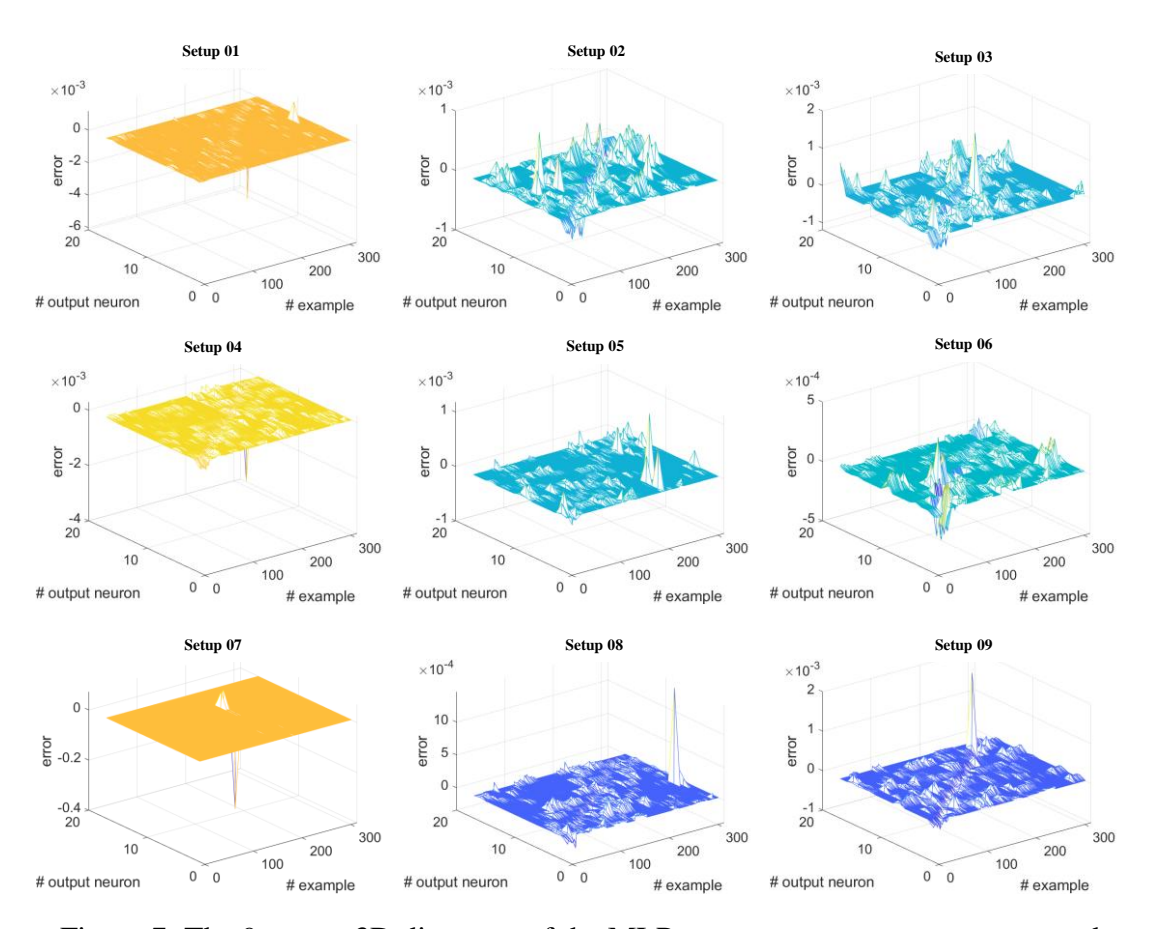


Figure 7: The 9 setups 3D diagrams of the MLP errors versus output neurons and examples of the test set.

It is worth noting that, when applied to actual online monitoring, cases like the one of Setup 07 may call for further checks. In fact, non-saturated values of the output could indicate an unknown class, namely the real scenario could belong to a class not represented in the training set. The most natural check in this case consists of verifying whether the same behaviour is confirmed or not in the previous or following instant. This could help to assess if the anomaly is due to a temporary disturbance.

The above considerations apply to the reliability assessment of the diagnosis provided by a single classifier. On the other hand, the 9 setups provide many

independent diagnoses that must be aggregated to obtain the final diagnosis. To this end, the majority voting method [22] was applied. The final classification was thus obtained by selecting the damage scenario that attained the majority of votes over the ensemble, thereby enhancing the robustness of the prediction. After several runs corresponding to different random selections of validation and test sets, at most one over the 9 MLPs was misclassified, demonstrating that the application of the majority voting method suitably leads to correctly classify 100% of the damage scenarios.

It is worthwhile to make a further remark concerning the capability of the classifier to distinguish between nominally equivalent scenarios. In particular, scenarios PD-02 and PD-08 are both undamaged scenarios, while scenarios from PD-03 to PD-07 are reversible (at least nominally). Nonetheless, the bridge's response was somehow affected by a sort of signature of the previous PDs, which made it possible to distinguish between scenarios PD-02 and PD-08. On the other hand, cumulative damage due to the application of successive PDs (as it occurs from PD-03 to PD-07) is detected by the MLP diagnostic system.

## **5** Conclusions and Contributions

The ability of structural health monitoring (SHM) in damage detection can be strengthened using artificial intelligence, which makes it possible to identify different kinds and levels of damage, even at their early stage. This paper presents a preliminary study to assess the effectiveness of a damage detection procedure based on training multi-layer perceptron (MLP) artificial neural networks (ANN) over SHM vibrational data. The data collected on the benchmark Z24 bridge during progressive damage (PD) tests is exploited to this purpose. The variety of acquisition setups and sensors, as well as the significant amount of damage scenarios, makes the Z24 bridge dataset particularly suitable for validating the proposed classification method.

A classification problem was solved, where each damage scenario represented a class. The experimental time signals obtained from different sensors setups and damage scenarios were pre-processed by applying synchronized sliding time windows and 2-dimensional fast Fourier transform (FFT). A specific MLP was trained for each setup, thus obtaining 9 different diagnostic systems. The set of diagnoses obtained from the different MLPs was finally combined with the majority voting criterion.

The results showed that the proposed procedure was able to recognize patterns in the vibration data that correspond to the different categories and severity of damage in the bridge. The diagnostic systems classified 100% of the test examples correctly, thus showing to be able to learn how to map selected features of the specific damage scenarios produced in the Z24 bridge test campaign. The results refer to a specific case study because of the enormous difficulty in finding large datasets of experimental vibration data relevant to a real structure under different damage scenarios. They are nonetheless sufficient to show the effectiveness of the simple MLP classifier in detecting the presence and categorize the type of damage, even being able to distinguish between different levels of damage of the same type.

The MLP ANN method here proposed has the advantage of being less computational expensive than other methods based on ANNs, while providing comparable good results (at least for the Z24 bridge). It could be applied to online monitoring of civil structures, which can be affected by many different categories and levels of damage. To make the MLP classifier an effective damage detection tool in current SHM practice, however, an identified twin numerical model of the actual structure should be implemented to train MLP neural networks on databases obtained from simulated damage test campaigns. The efficacy of the diagnostic system strictly depends on the reliability of such numerical model. Future studies will be devoted to developing this part of the study.

# Acknowledgements

The authors acknowledge the structural mechanics section of KU Leuven for granting access to the Z24 bridge benchmark dataset. Professor Emeritus Guido De Roeck is also gratefully acknowledged for permitting the use of Z24 bridge images.

## References

- [1] J. Seo, J. W. Hu, and J. Lee, 'Summary Review of Structural Health Monitoring Applications for Highway Bridges', J. Perform. Constr. Facil., vol. 30, no. 4, p. 04015072, Aug. 2016, doi: 10.1061/(ASCE)CF.1943-5509.0000824.
- [2] M. C. Porcu, M. Buitrago, P. A. Calderón, M. Garau, M. F. Cocco, and J. M. Adam, 'Robustness-based assessment and monitoring of steel truss railway bridges to prevent progressive collapse', J. Constr. Steel Res., vol. 226, p. 109200, Mar. 2025, doi: 10.1016/j.jcsr.2024.109200.
- [3] G. Caredda, M. C. Porcu, M. Buitrago, E. Bertolesi, and J. M. Adam, 'Analysing local failure scenarios to assess the robustness of steel truss-type bridges', Eng. Struct., vol. 262, p. 114341, Jul. 2022, doi: 10.1016/j.engstruct.2022.114341.
- [4] M. C. Porcu, D. M. Patteri, S. Melis, and F. Aymerich, 'Effectiveness of the FRF curvature technique for structural health monitoring', Constr. Build. Mater., vol. 226, pp. 173–187, Nov. 2019, doi: 10.1016/j.conbuildmat.2019.07.123.
- [5] R. Zinno, S. S. Haghshenas, G. Guido, and A. VItale, 'Artificial Intelligence and Structural Health Monitoring of Bridges: A Review of the State-of-the-Art', IEEE Access, vol. 10, pp. 88058–88078, 2022, doi: 10.1109/ACCESS.2022.3199443.
- [6] C. Calledda, A. Montisci, and M. C. Porcu, 'Optimal Design of Earthquake-Resistant Buildings Based on Neural Network Inversion', Appl. Sci., vol. 11, no. 10, p. 4654, May 2021, doi: 10.3390/app11104654.
- [7] J. Maeck and G. De Roeck, 'DESCRIPTION OF Z24 BENCHMARK', Mech. Syst. Signal Process., vol. 17, no. 1, pp. 127–131, Jan. 2003, doi: 10.1006/mssp.2002.1548.
- [8] S. Sony, S. Gamage, A. Sadhu, and J. Samarabandu, 'Multiclass Damage Identification in a Full-Scale Bridge Using Optimally Tuned One-Dimensional Convolutional Neural Network', J. Comput. Civ. Eng., vol. 36, no. 2, p. 04021035, Mar. 2022, doi: 10.1061/(ASCE)CP.1943-5487.0001003.

- [9] A. Dabbous, R. Berta, M. Fresta, H. Ballout, L. Lazzaroni, and F. Bellotti, 'Bringing Intelligence to the Edge for Structural Health Monitoring: The Case Study of the Z24 Bridge', IEEE Open J. Ind. Electron. Soc., vol. 5, pp. 781–794, 2024, doi: 10.1109/OJIES.2024.3434341.
- [10] V. H. Hoang, N. L. Nguyen, T. T. Bui, and N. H. Tran, 'A Two-stage Method for Damage Detection in Z24 Bridge Based on K-nearest Neighbor and Artificial Neural Network', Period. Polytech. Civ. Eng., vol. 68, no. 3, pp. 892–902, Apr. 2024, doi: 10.3311/PPci.23884.
- [11] V. Giglioni, I. Venanzi, V. Poggioni, A. Baia, A. Milani, and F. Ubertini, 'Deep neural networks for unsupervised damage detection on the Z24 bridge', in 8th European Congress on Computational Methods in Applied Sciences and Engineering, CIMNE, 2022. doi: 10.23967/eccomas.2022.080.
- [12] H. Nguyen-Tran et al., 'The Application of a Hybrid Autoregressive and Artificial Neural Networks to Structural Damage Detection in Z24 Bridge', in Recent Advances in Structural Health Monitoring and Engineering Structures, R. V. Rao, S. Khatir, and T. Cuong-Le, Eds., in Lecture Notes in Mechanical Engineering., Singapore: Springer Nature Singapore, 2023, pp. 417–425. doi: 10.1007/978-981-19-4835-0\_36.
- [13] O. R. de Lautour and P. Omenzetter, 'Nearest neighbor and learning vector quantization classification for damage detection using time series analysis', Struct. Control Health Monit., vol. 17, no. 6, pp. 614–631, 2010, doi: 10.1002/stc.335.
- [14] M. L. Foddis, P. Ackerer, A. Montisci, and G. Uras, 'ANN-based approach for the estimation of aquifer pollutant source behaviour', Water Supply, vol. 15, no. 6, pp. 1285–1294, Dec. 2015, doi: 10.2166/ws.2015.087.
- [15] R. Secci, M. Laura Foddis, A. Mazzella, A. Montisci, and G. Uras, 'Artificial Neural Networks and Kriging Method for Slope Geomechanical Characterization', in Engineering Geology for Society and Territory Volume 2, G. Lollino, D. Giordan, G. B. Crosta, J. Corominas, R. Azzam, J. Wasowski, and N. Sciarra, Eds., Cham: Springer International Publishing, 2015, pp. 1357–1361. doi: 10.1007/978-3-319-09057-3\_239.
- [16] M. L. Foddis, A. Montisci, F. Trabelsi, and G. Uras, 'An MLP-ANN-based approach for assessing nitrate contamination', Water Supply, vol. 19, no. 7, pp. 1911–1917, Nov. 2019, doi: 10.2166/ws.2019.066.
- [17] C. Krämer, C. A. M. De Smet, and G. De Roeck, 'Z24 bridge damage detection tests', in IMAC 17, the International Modal Analysis Conference, Kissimee, Fl, USA: Society of Photo-optical Instrumentation Engineers, 1999, pp. 1023–1029.
- [18] G. De Roeck, 'SIMCES Synthesis Report', BRITEEuram BE96-3157 Kathol. Univ. Leuven, 1999.
- [19] G. D. Roeck, 'The state-of-the-art of damage detection by vibration monitoring: the SIMCES experience', J. Struct. Control, vol. 10, no. 2, pp. 127–134, Apr. 2003, doi: 10.1002/stc.20.
- [20] B. Peeters, 'System identification and damage detection in civil engeneering', PhD thesis, Katholieke Universiteit te Leuven, 2000.

- [21] MATLAB version: 24.2 (R2024b). (Sep. 12, 2024). The MathWork Inc., Natick, Massachussets. [Online]. Available: https://www.mathworks.com
- [22] A. Rojarath, W. Songpan, and C. Pong-inwong, 'Improved ensemble learning for classification techniques based on majority voting', in 2016 7th IEEE International Conference on Software Engineering and Service Science (ICSESS), Beijing, China: IEEE, Aug. 2016, pp. 107–110. doi: 10.1109/ICSESS.2016.7883026.